Cavity-enhanced on-chip absorption spectroscopy using microring resonators

Arthur Nitkowski[1], Long Chen[2], and Michal Lipson[2,*]

[1]*School of Applied and Engineering Physics, Cornell University, Ithaca, NY 14853*
[2]*School of Electrical and Computer Engineering, Cornell University, Ithaca, NY 14853*
[*]*Corresponding author: lipson@ece.cornell.edu*

Abstract: We demonstrate on-chip laser absorption spectroscopy using silicon microring resonators integrated with PDMS microfluidic channels. A 100 μm radius microring resonator with Q > 100,000 is used to enhance the interaction length between evanescent light and a cladding liquid. We measure absorption spectra of less than 2 nL of N-methylaniline from 1460 nm to 1610 nm with 1 nm resolution and effective free space path lengths up to 5 mm. This work can help realize a completely on-chip spectroscopy device for lab-on-a-chip applications.

OCIS codes: (130.6010) Integrated Optics: Sensors; (300.1030) Spectroscopy: Absorption.

References and links

1. D. Psaltis, S. R. Quake, and C. H. Yang, "Developing optofluidic technology through the fusion of microfluidics and optics," Nature **442**, 381-386 (2006).
2. D. Erickson, S. Mandal, A. H. J. Yang, and B. Cordovez, "Nanobiosensors: optofluidic, electrical and mechanical approaches to biomolecular detection at the nanoscale," Microfluid. Nanofluid. **4**, 33-52 (2008).
3. C. Y. Chao, W. Fung, and L. J. Guo, "Polymer microring resonators for biochemical sensing applications," IEEE J. of Sel. Top. Quantum Electron. **12**, 134-142 (2006).
4. J. J. Hu, V. Tarasov, A. Agarwal, L. Kimerling, N. Carlie, L. Petit, and K. Richardson, "Fabrication and testing of planar chalcogenide waveguide integrated microfluidic sensor," Opt. Express **15**, 2307-2314 (2007).
5. M. L. Chabinyc, D. T. Chiu, J. C. McDonald, A. D. Stroock, J. F. Christian, A. M. Karger, and G. M. Whitesides, "An integrated fluorescence detection system in poly(dimethylsiloxane) for microfluidic applications," Anal. Chem. **73**, 4491-4498 (2001).
6. J. Dostalek, J. Ctyroky, J. Homola, E. Brynda, M. Skalsky, P. Nekvindova, J. Spirkova, J. Skvor, and J. Schrofel, "Surface plasmon resonance biosensor based on integrated optical waveguide," Sens. Actuators B **76**, 8-12 (2001).
7. K. Schmitt, B. Schirmer, C. Hoffmann, A. Brandenburg, and P. Meyrueis, "Interferometric biosensor based on planar optical waveguide sensor chips for label-free detection of surface bound bioreactions," Biosens. Bioelectron. **22**, 2591-2597 (2007).
8. W. G. Yang, D. B. Conkey, B. Wu, D. L. Yin, A. R. Hawkins, and H. Schmidt, "Atomic spectroscopy on a chip," Nat. Photonics **1**, 331-335 (2007).
9. N. A. Mortensen, S. S. Xiao, and J. Pedersen, "Liquid-infiltrated photonic crystals: enhanced light-matter interactions for lab-on-a-chip applications," Microfluid. Nanofluid. **4**, 117-127 (2008).
10. A. R. Hawkins and H. Schmidt, "Optofluidic waveguides: II. Fabrication and structures," Microfluid. Nanofluid. **4**, 17-32 (2008).
11. R. W. Boyd and J. E. Heebner, "Sensitive disk resonator photonic biosensor," Appl. Opt. **40**, 5742-5747 (2001).
12. G. Farca, S. I. Shopova, and A. T. Rosenberger, "Cavity-enhanced laser absorption spectroscopy using microresonator whispering-gallery modes," Opt. Express **15**, 17443-17448 (2007).
13. A. M. Armani and K. J. Vahala, "Heavy water detection using ultra-high-Q microcavities," Opt. Lett. **31**, 1896-1898 (2006).
14. M. A. Belkin, M. Loncar, B. G. Lee, C. Pflugl, R. Audet, L. Diehl, F. Capasso, D. Bour, S. Corzine, and G. Hofler, "Intra-cavity absorption spectroscopy with narrow-ridge microfluidic quantum cascade lasers," Opt. Express **15**, 11262-11271 (2007).
15. A. Yariv, "Universal relations for coupling of optical power between microresonators and dielectric waveguides," Electron. Lett. **36**, 321-322 (2000).
16. A. Yariv, "Critical coupling and its control in optical waveguide-ring resonator systems," IEEE Photon. Technol. Lett. **14**, 483-485 (2002).
17. P. Rabiei, W. H. Steier, C. Zhang, and L. R. Dalton, "Polymer micro-ring filters and modulators," J. Lightwave Technol. **20**, 1968-1975 (2002).

#96529 - $15.00 USD Received 21 May 2008; revised 17 Jul 2008; accepted 18 Jul 2008; published 25 Jul 2008

18. J. T. Robinson, L. Chen, and M. Lipson, "On-chip gas detection in silicon optical microcavities," Opt. Express **16**, 4296-4301 (2008).

1. Introduction

Optofluidic techniques where microfluidics are integrated with photonic components are gaining widespread use in biosensing and chemical analysis applications [1]. Incorporating advanced fluid handling techniques at the micron scale with highly sensitive photonic devices has the potential to provide compact, effective sensors for lab-on-a-chip tools [2]. Many optofluidic transduction methods for sensing and analysis have been demonstrated including refraction [3], absorbance [4], fluorescence [5], surface-plasmon-resonance [6], and interferometric [7] measurements. Absorbance-based optofluidic techniques are particularly attractive since they offer the potential to provide label-free spectral information for detection and identification of an analyte [8]. However, the miniaturization of microfluidic devices reduces the optical path length for absorption based sensors as compared to macroscopic experiments. A shortened optical path reduces the interaction length of light with a fluid and thus limits the sensitivity of a device and its ability to detect an absorbing species. Several methods have been proposed to mitigate this problem including using slow-light in photonic crystals [9] or novel waveguide geometries [10]. It has been shown that high quality factor cavities, both passive [11-13] and active [14], can be used to enhance the interaction length between the guided light and an analyte. Previous work has required large scale components thus negating much of the benefit of using a microresonator or has involved detection at a particular wavelength thus providing little spectral information. In this work we demonstrate both integrated and broadband absorption spectroscopy in the near infrared using microring resonators and microfluidic channels.

2. Device design and fabrication

The proposed device is a silicon microring resonator covered by a microfluidic channel, as shown in Fig. 1(a). We design the device so that the evanescent light traveling in the ring resonator interacts with the upper fluidic cladding. At resonance, light circulates many times within the ring which leads to a large enhancement in the interaction length between the evanescent field and the cladding liquid. Any losses present in the fluid will alter the quality factor and extinction ratio of the transmission resonance. By extracting the absorption contribution of an analyte to a resonance and repeating this process for many resonances over a range of wavelengths, an absorption spectrum for an analyte can be measured.

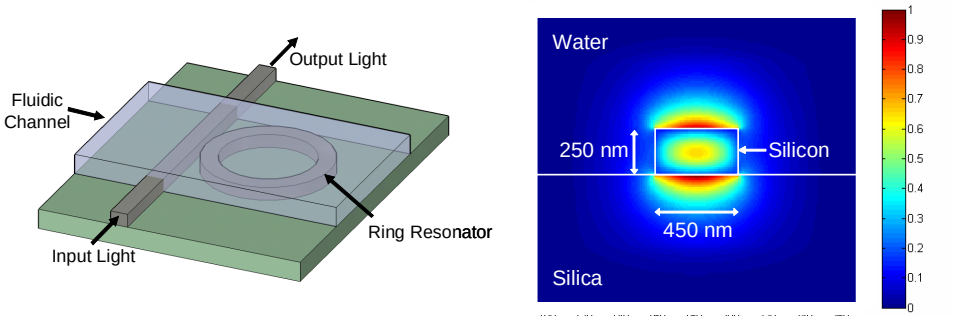

(a) (b)

Fig. 1. (a). Illustration of our device design with a straight waveguide coupled to a ring resonator and a microfluidic channel on top. (b) The electric field mode profile for the quasi TM mode propagating in a silicon waveguide in an aqueous environment.

The device was designed to maximize interaction with the cladding fluid. The cross section of the ring and waveguide are 450 nm wide by 250 nm tall which supports a single

#96529 - $15.00 USD Received 21 May 2008; revised 17 Jul 2008; accepted 18 Jul 2008; published 25 Jul 2008

mode at 1.5 μm. The resolution of our absorption spectroscopy device is determined by the free spectral range between resonances, therefore the ring radius (100 μm) was chosen to provide a FSR of ~1 nm. The E_y mode profile for quasi TM polarized light with an aqueous upper cladding is shown in Fig. 1(b). The coupling distance between the bus waveguide and ring is 300 nm. The straight waveguides are oxide clad which provides a symmetric index profile to increase optical fiber input light coupling and also reduces waveguide losses. The ring resonators are exposed (uncladded) which allows maximum interaction of the evanescent light trapped in the ring with any subsequent fluidic cladding.

The optical structure was fabricated using standard microfabrication techniques on a silicon-on-insulator wafer with a 3 μm buried oxide layer and 250 nm device layer. The devices were patterned with a JEOL electron beam lithography system and then etched using inductively coupled plasma etching. Lift-off resist and then photoresist were spun onto the wafer and patterned using contact lithography to mask the ring resonators. A 1.7 μm cladding layer of silicon dioxide was then evaporated over the wafer using an electron gun source and cryopumped evaporator. After dicing and polishing, the oxide and resist over the ring resonator were removed using Microposit Remover 1165 leaving the ring exposed (Fig. 2(a)).

The microfluidic channels were made from PDMS using soft lithography processes. A master mold for the microfluidic channels was made by spin-coating SU-8 photoresist to a thickness of 30 μm on a silicon wafer. Using contact lithography, channels with a width of 300 μm were patterned onto the SU-8 including alignment marks to later align the channels to the photonic devices. PDMS was then poured over the mold and baked at 80°C for several hours. The PDMS was then cut and peeled off the master wafer and holes were punched through the PDMS to act as inlet and outlet ports for fluids. The chip and fluidics layer were then oxygen plasma cleaned before a contact aligner was used to irreversibly bond the PDMS to our device chip. Finally, we connect Tygon tubing to the microfluidic channel inlets to allow fluid to be introduced into the channel. The completed device is shown in Fig. 2(b) and includes over 50 waveguides and ring resonators with their output offset by 3 mm to prevent input light from scattering into the output light detector. A microfluidic channel connects the two inlets (highlighted in yellow in Fig. 2(b)) and crosses the ring resonators that are coupled to each waveguide. The required volume of fluid to cover a single ring resonator with the channel size used for this device is less than 2 nL.

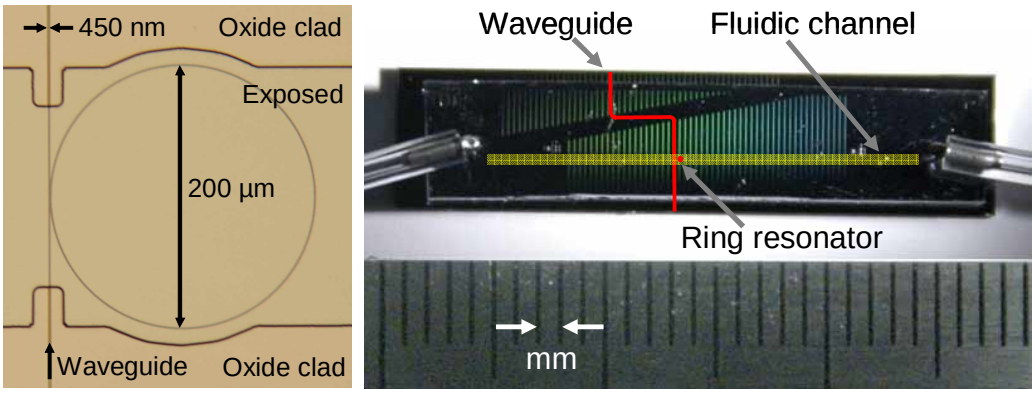

(a) (b)

Fig. 2. (a). Optical microscope image of the fabricated structure consisting of an exposed silicon microring resonator and an oxide clad bus waveguide. (b) Complete device with an integrated PDMS microchannel spanning 50 waveguides with ring resonators.

#96529 - $15.00 USD Received 21 May 2008; revised 17 Jul 2008; accepted 18 Jul 2008; published 25 Jul 2008

3. Methods

The experimental procedure for extracting the spectral information of the analyte consists of tuning the wavelength of the input light source while recording the transmission of the bus waveguide for various fluids present in the microfluidic channel. The setup includes a tunable laser source (Tunics Reference SCL) which is coupled into our waveguides using a tapered lens fiber to increase coupling efficiency. Transmission through the device is collected with a microscope objective lens and focused onto a photo-detector. Voltage outputs from both the power meter and laser source are sent to a DAQ card (National Instruments USB-6009) and recorded and synchronized by a computer running a LabView (National Instruments) script. The laser is tuned continuously at 1 nm/sec from 1460 nm to 1610 nm and the power meter samples the detector at 500 Hz resulting in a spectrum resolution of 2 pm. The acquisition time for this 150 nm window is 2.5 minutes; however this can be greatly reduced by using a faster detector. With a 50 KHz detector and a maximum laser sweep speed of 100 nm/sec, the acquisition time would be reduced to 1.5 seconds while maintaining 2 pm resolution. The fluids of interest are controlled by pressure driven flow from a syringe pump (NE-1000 from New Era Pump Systems, Inc). The photonic chip is placed on a thermo-electric cooler to maintain temperature stability.

To determine the loss contribution of the analyte from the recorded transmission resonance curve, the following method is employed. Resonance in the ring corresponds to a dip in the transmission through the straight waveguide due to destructive interference between the transmitted light and ring light coupling back into the straight waveguide. The transmission at resonance is given by [15]:

$$T(\theta) = \frac{a^2 + |t|^2 - 2a|t|\cos\theta}{1 + a^2|t|^2 - 2a|t|\cos\theta} \tag{1}$$

where a is the field attenuation coefficient, t is the field transmission coefficient at the waveguide/ring coupling region, and θ is the phase shift per circulation. The phase shift can be expressed in terms of the free space wavelength as $\theta = 2\pi L n_{eff}/\lambda$ where L is the ring circumference and n_{eff} is the effective index of the mode [16]. It is beneficial to restate Eq. (1) in terms of experimentally measurable quantities so that the only fitting parameters are the attenuation and transmission coefficients. This can be done by expanding the cosine term in Eq. (1) for small wavelength deviations around a resonant wavelength λ_o:

$$\cos(\theta) = \cos(2\pi L n_{eff}/\lambda) \cong 1 - \frac{2\pi^2 L^2 n_g^2}{\lambda_o^4}(\lambda - \lambda_o)^2 \tag{2}$$

where L is the ring circumference and the group index n_g can be calculated directly from the resonance spacing using the relation $FSR = \lambda^2 / n_g L$ [17].

Fitting the theoretical curve described by Eq. (1) to a resonance yields values for the attenuation and transmission coefficients. However, since these coefficients are interchangeable in Eq. (1) they need to be distinguished. This can be done by comparing the coefficient values for two rings of equal radius but with different size gaps between the ring and bus waveguide. The field transmission coefficients which describe coupling will shift to lower values (greater coupling) for smaller gap distances while the attenuation coefficients remain the same. The total absorption coefficient α_T for propagation within the ring is then determined from the relation $a = \exp(-\alpha_T L/2)$. The total absorption is related to the absorption of the fluid by

$$\alpha_T = \alpha_I + \Gamma \alpha_A \tag{3}$$

#96529 - $15.00 USD Received 21 May 2008; revised 17 Jul 2008; accepted 18 Jul 2008; published 25 Jul 2008

where α_I is the intrinsic waveguide loss, α_A is the absorption from the analyte, and Γ is the confinement factor which is a measure of how much of the total guided light is interacting with the cladding material. The confinement factor can be determined from a simulation of a waveguide's mode profile using[18]:

$$\Gamma = \frac{n_A \int_A |\boldsymbol{E}|^2 dA}{Z_o \int_\infty \mathrm{Re}\left\{ \boldsymbol{E} \times \boldsymbol{H}^* \right\} \cdot \hat{\boldsymbol{z}}\, dA} \tag{4}$$

where the top integral is over the analyte cladded region, n_A is the refractive index of the analyte and Z_o is the free space impedance.

4. Results and discussion

In order to measure the absorption spectrum of an analyte, we first perform measurements with no fluid in the channel (air exposed devices) to determine the intrinsic waveguide loss, α_I. We chose to make this measurement with no fluid in the channel both for simplicity and because the change in coupling due to the addition of a fluid will not significantly alter the intrinsic waveguide loss. We measure the transmission through the device and analyze each resonance to determine the waveguide loss over the spectral range of our tunable source. An example of the curve fitting can be seen in Fig. 3 which shows a loaded Q value of ~120,000. Using the methods described above, the resonance is known to be slightly undercoupled and the resulting fitting parameters are t=0.981 and a=0.967 for the field transmission and attenuation coefficients respectively. The attenuation value for this resonance corresponds to an intrinsic waveguide absorption of $\alpha_I = 1.07\ cm^{-1} = 4.67\ dB/cm$ for waveguide propagation.

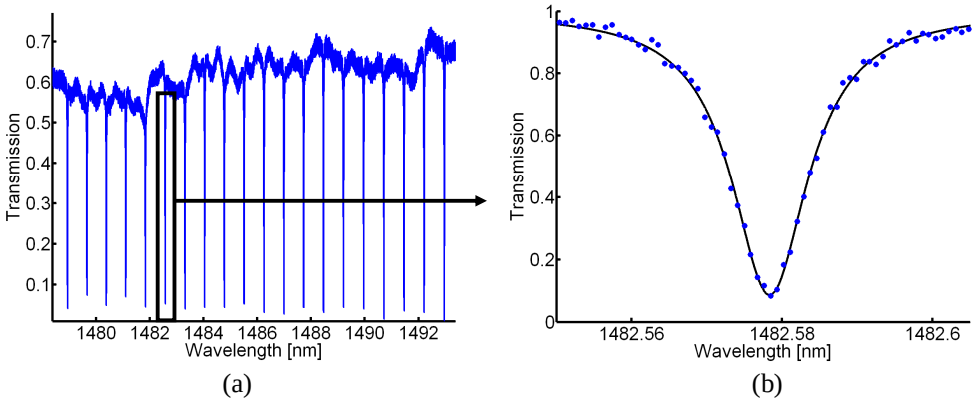

Fig. 3. (a). Ring resonator transmission showing a 15 nm window of the complete transmission spectrum (1460 nm – 1610 nm). (b) A close up of a representative resonance dip (points) and the resulting curve fitting (solid line). The waveguide loss at the resonance wavelength is 4.67 dB/cm and the resonance has a quality factor of 120,000.

We demonstrate the ability to detect absorption features in an analyte by injecting pure N-methylaniline into the microfluidic channels. This analyte was chosen since the N-H bonds in N-methylaniline lead to an absorption peak near 1500 nm [4] which is within the limits of our tunable laser. The FSR between resonances is ~1 nm and each resonance is fitted to determine the attenuation and transmission coefficient, shown in the inset of Fig. 4. Once the total absorption is known, we determine the contribution from the fluid using Eq. (3) and subtracting the intrinsic absorption measured while the device is air clad. The confinement factor for our waveguide dimensions was calculated from Eq. (4) using a refractive index of 1.56 for N-methylaniline. The absorption spectrum of N-methylaniline measured using the ring resonator device is plotted in Fig. 4 along with the absorption measured using a

#96529 - $15.00 USD Received 21 May 2008; revised 17 Jul 2008; accepted 18 Jul 2008; published 25 Jul 2008

commercial spectrophotometer **(**Shimadzu UV-3101PC UV/Vis/Near-IR Spectrophotometer) and there is very good agreement between the two curves. The results plotted in Fig. 4 are the average of 8 consecutive measurements for a single microring resonator with an average standard deviation of 0.25 cm^{-1}. The additional noise present at the absorption peak is likely due to the decrease in the extinction ratio of the resonances at these wavelengths which lowers the signal to noise ratio of the measurement.

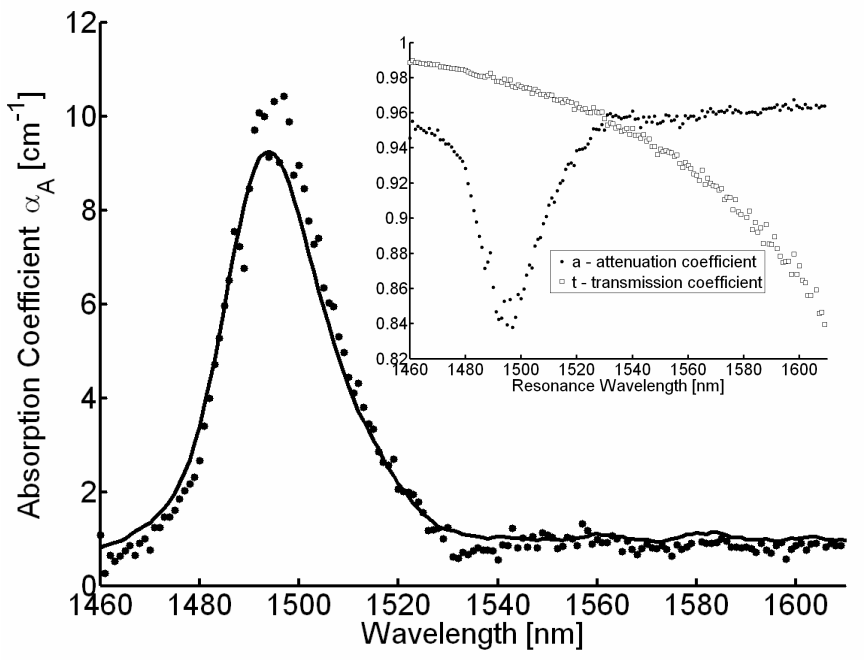

Fig. 4. Absorption spectrum for N-methylaniline measured using a microring resonator (points) and with a commercial spectrophotometer (solid line). The inset shows the attenuation and transmission coefficients for each resonant wavelength.

The sensitivity of the device is related to the effective path length traveled by light circulating within the ring. The free space equivalent path length can be determined from the quality factor Q of the ring resonance as $L_{eff} = \Gamma \frac{Q\lambda_o}{2\pi n_{eff}}$. For the resonance measured in our device with a Q~120,000, effective index of 2.5, and confinement factor of 0.43, the calculated effective path length is ~5 mm. A straight waveguide without a ring would have to be ~20 times longer to achieve the same sensitivities which shows that microring resonators can be effectively used to increase the sensitivity of a miniaturized on-chip device.

The resolution of measurements with our device is determined by the FSR between resonance wavelengths. The FSR is dependent on the ring circumference which can be lengthened if higher resolution is required or shortened to make the device more compact. With a 1 nm FSR, the resolution of our device is higher than that of the spectrophotometer used as a comparison in Fig. 4 which had a minimum slit width of 2 nm. The resolution of a straight waveguide would be only limited by the linewidth of the laser but this increased resolution comes with the cost of reduced sensitivity as mentioned earlier.

Another important quantity for determining the quality of a spectroscopy measurement is the signal to noise ratio (SNR). The light source, detector and coupling into the photonic chip contribute to the noise of a measurement. The first two sources are present for any spectrometer measurement while the third contribution is unique to integrated photonic devices. Coupling noise is due to both mechanical vibrations as well as reflections from the end facets which lead to Fabry-Perot noise at the output. The SNR of a signal from our laser

#96529 - $15.00 USD Received 21 May 2008; revised 17 Jul 2008; accepted 18 Jul 2008; published 25 Jul 2008

source to the detector is ~50 dB. With coupling into a photonic chip, the SNR is reduced to ~43 dB. This additional source of noise for photonic devices due to coupling could be eliminated by using an integrated light source and detector which would allow the SNR of the measurement to approach that of commercial spectrophotometers.

5. Conclusion

In this work we have demonstrated cavity-enhanced absorption of an analyte with an integrated on-chip device. A 100 μm radius microring resonator with Q values > 100,000 was used to measure the absorption spectra of N-methylaniline from 1460 to 1610 nm with a resolution of 1 nm. The wavelength range of the device was limited by laser tunability and in principle measurements could be extended from 1.2 to 6 μm using silicon waveguides with an appropriate buried oxide thickness. We have shown good agreement between measurements with a commercial spectrophotometer and the extracted absorption using our device with less than 2 nL of fluid and a device footprint of less than 0.03 mm^2. While the infrared wavelength range is useful for spectroscopy applications for chemical analysis, it would also be beneficial to extend this technique into the UV/Vis spectrum for biological analyte measurements. Similar measurement could be performed with waveguides and resonators made using silicon nitride (Si_3N_4) which is transparent in the visible spectrum. This technique can help realize a completely on-chip spectroscopy device for label-free massively parallel detection of analytes for lab-on-a-chip applications.

Acknowledgments

The authors gratefully acknowledge David Erickson for the use of his microfluidic fabrication facilities and Christina Manolatou for the use of her finite difference mode solver. This material is based on work supported by the IGERT Program of the National Science Foundation under Agreement No. DGE-0654112, administered by the Nanobiotechnology Center at Cornell. This work was performed in part at the Cornell NanoScale Facility, a member of the National Nanotechnology Infrastructure Network, which is supported by the National Science Foundation.

#96529 - $15.00 USD Received 21 May 2008; revised 17 Jul 2008; accepted 18 Jul 2008; published 25 Jul 2008